17th World Conference on Earthquake Engineering, 17WCEE
Sendai, Japan - September 13th to 18th 2020

PARAMETRIC STUDY ON SEISMIC PERFORMANCE OF SELF-CENTERING PRECAST CONCRETE WALLS WITH MULTIPLE ROCKING JOINTS

H. Wu[(1)], Y. Zhou[(2)]

[(1)] *Assistant Researcher, Tongji University, 2009wuhao_tom@tongji.edu.cn*
[(2)] *Professor, Tongji University, yingzhou@tongji.edu.cn*

Abstract

Previous research has demonstrated superior performance of self-centering precast concrete wall system that has a base-rocking mechanism to limit seismic forces at wall base without accepting significant damage. In addition, this wall system utilizes self-centering mechanisms (e.g. post-tensioning) to limit residual drifts after large lateral excursion. However, the self-centering precast wall system is limited in height because of amplified upper wall panel forces that are induced by higher-mode effects. A possible way to mitigate this effects is to introduce additional rocking joints in the upper stories. Although the utilize of multiple rocking joints to control wall upper panel forces is easily to be understood, the effects of different wall design parameters on the efficiency of mitigating higher-mode response as well as the overall seismic performance are still unclear. To this end, a parametric study is conducted in this paper to investigate the effects for a series of design parameters on the seismic performance of self-centering precast concrete walls with multiple rocking joints. The parameter variations include different rocking joint locations, number of upper story rocking joints, wall heights, energy dissipation levels, yielding forces of energy dissipators, etc. Three prototype self-centering precast wall structures have been designed with various design parameters, then the analytical models are established for the prototype structures considering different multiple rocking joint configurations. A selection of 20 earthquake ground motions is used for nonlinear response history analyses for the established models. Statistical results prove that the force envelopes above the base of self-centering precast walls can be significantly reduced by introducing multiple rocking joints over the wall heights, while the energy dissipation level from the upper wall joints is not evidently useful in mitigating wall forces as well as displacements. The relations between different design parameters and the overall structural responses are also revealed in the study.

Keywords: self-centering wall, multiple rocking joints, seismic performance, parametric analysis

1. Introduction

In the past decades, the design philosophy in earthquake engineering has been changed from preventing buildings from collapse to reducing repair cost and downtime after a severe earthquake event [1-3]. This new philosophy focuses on developing innovative structural systems that would minimize structural damage and residual deformation, thus allowing buildings to be reused or repaired quickly after earthquake. One class of such new systems is the self-centering precast concrete wall [4-6] which typically relies on a rocking mechanism at wall base to mitigate high force demands that otherwise should be experienced by the traditional reinforced concrete walls. As the schematic concept shown in **Fig. 1**, the self-centering precast wall is normally designed with a rocking joint at wall base, allowing it to rock back and forth (wall uplift at base) during earthquake. The lateral resistance for the base rocking joint is typically provided by a combination of high-strength unbonded post-tensioned (PT) steel and energy dissipation (ED) devices (e.g. mild ED bars). The longitudinal rebars in the wall panels are not continuous at the rocking joint. A characteristic flag-shaped hysteretic response is expected by reasonably proportioning the relative amount of PT and ED components, which make the wall has limited residual deformation after large lateral excursion (i.e., self-centering). The dominant displacement mode for such walls under lateral loads occurs through gap opening at the rocking joint, allowing the wall to undergo large inelastic drifts without significant damage to wall panels (or much less evident damage as compared to conventional RC walls).

Previous research on self-centering precast walls has been conducted extensively, and have demonstrated the excellent performance of such systems under earthquake loading. Most of the research in the past have been focused on investigating the seismic behavior of single or coupled self-centering walls under static cyclic loading [7-12] or dynamic earthquake loading [13-16]. Note that most of the previous self-centering walls considered (both experimentally and analytically) were designed only with a single base rocking joint. One of the challenges in adopting self-centering walls into the engineering practice is the higher mode effects that may occur for tall buildings, causing amplified seismic demands over building height. The past research has already demonstrated the unneglectable higher mode effects for base-yielding systems [17], and this may also occur to the self-centering walls with single base rocking joint [18-19]. Similar to the base rocking concept, a possible way to mitigate the higher mode forces is to introduce additional rocking joints at the upper stories, i.e., walls with multiple rocking joints. Although the concept is clear and should be acceptable, the effects of different wall design parameters on the efficiency of multiple-rocking-joint-mechanism in mitigating seismic demands is still doubtful. To this end, a parametric study is conducted in this study to investigate the influences of different design parameters on the seismic performance of self-centering walls with multiple rocking joints.

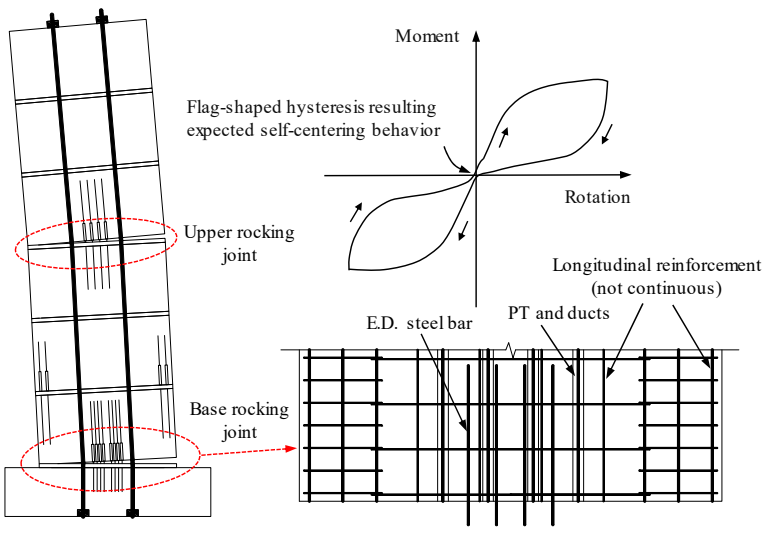

Fig. 1 – Concept of self-centering precast walls with multiple rocking joints

2. Prototype wall design and ground motions

2.1 Prototype wall buildings

To evaluate the effects of multiple rocking joint mechanism for self-centering walls, three idealized prototype office buildings of 6-, 9-, and 12-story was designed. **Fig. 2** shows the building plan view. As shown, the building has a 5 by 3 bay plan with bay width of 9.0 m in the longitudinal direction and 6.0 m in the transverse direction. The lateral force resistance in the longitudinal direction is provided by moment resisting frames, while the resistance in the transvers direction is provided by self-centering walls. All the prototype buildings have a same plan view, except that the wall number is different, i.e., 2-, 4-, and 6-walls are used for the 6-, 9-, and 12-story buildings, respectively. For each building, the self-centering precast walls are designed to resist all the seismic actions in the transverse direction, while the gravity load of the building is assumed to be resisted by the gravity frames only. To simplify the design process, the interaction effects between a self-centering wall and the floor diaphragm [20-21] has been neglected. The current study only focuses on evaluating the performance of walls.

The prototype buildings are assumed to be located on a stiff soil site in San Francisco, USA. The specific site-related seismic design factors are the similar as that in the previous study [22]. The design dead and live loads are assumed to be 6.5 kN/m^2 and 2.0 kN/m^2, respectively, for both floor and roof. Design of the prototype buildings is in accordance with the classic force-method as prescribed in ASCE/SEI 7-10 [23]. Part of the critical design parameters include: seismic design category of "D"; response reduction factor R of 6; S_{DS} = 1.0 g, S_{D1} = 0.643 g, T_0 = 0.129 sec and T_S = 0.643 sec for 5% damped design-based-earthquake (DBE) response spectrum. The maximum considered earthquake (MCE) level spectrum is 1.5 times that of DBE. Note that both DBE and MCE level earthquakes have been considered in the study, but only the MCE responses would be presented in the current paper for brief.

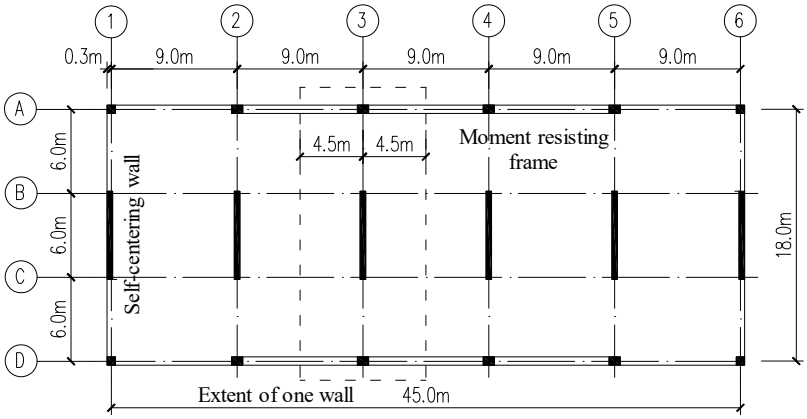

Fig. 2 – Building plan view (9-story building with 6 walls)

2.2 Design of self-centering precast walls

Unlike conventional RC walls, moment resistance of a self-centering precast wall is provided by a combination of PT steel and energy dissipators (e.g., mild ED rebar in this case). Therefore, the nominal base moment resistance (M_n) of a self-centering wall consists of three components, namely M_s, M_p, and M_g, representing the moment contributions from mild ED steel, PT steel and applied external axial loads, respectively, as shown in Eq. (1). Through selecting and positioning different PT steel and ED steel, the designers could have a large control over the hysteretic behavior of the system. Therefore, the current study utilizes various wall designs with varying design parameters to investigate their influences on the overall behavior of the target system.

$$M_n = M_s + M_p + M_g \quad (1)$$

The design of the self-centering walls are based on the walls with base rocking (BR) joint only, and the design parameters for the walls with multiple rocking (MR) joints could be modified easily afterwards.

The walls (BR6, BR9, and BR12) are designed to meet the minimum required base moment demand according to ACI ITG-5.2-09 [24] and ACI 318-11 [25]. The primary design parameters and section reinforcements of the walls are summarized in **Table 1**. Note that all the walls for the three prototype buildings have a same section dimension of 6.3 m in length and 0.4 m in thickness. The cylinder stresses of unconfined and confined concrete for the walls are 41.4 MPa and 69.0 MPa, respectively, and the yielding stress of 455 MPa for the ED rebar, and ultimate stress of 1862 MPa for PT steel. Similar as in the previous research [22], shear deformation is not considered in design or analyzed in the study. However, shear deformation should be carefully considered in real engineering practice.

The three base rocking wall models (BR3~BR6) are served as the baseline models in the study. The design parameters utilized are relatively optimal, such as κ, total moment capacity as shown in **Table 1**. The current study focuses on the parametric analysis of self-centering walls incorporating multiple rocking joints in the upper panels, and the main objective of the study is to investigate the overall design parameters on the effects of seismic response mitigation from using additional rocking joints. These overall parameters for the walls are in more general respect, such as yielding capacity and energy dissipation level of the rocking joint. To simplify the modeling process and facilitate the analysis, a simple spring model would be used in the analysis as addressed later in Section 3. The simple model requires a general input for the rocking joint modeling, rather than the precise input of parameters from other modeling method (e.g., fiber models). To this end, the specific design of the upper rocking joint (reinforcement design) is not performed in the study, and a general proportion factor in respective to that of the base rocking joint would be instead used in the models for parametric analyses.

Table 1 – Design parameters of baseline wall models

Wall ID	H_w (m)	M_{DES} (kN·m)	PT steel		ED steel		M_g (kN·m)	κ
			Configuration	M_p (kN·m)	Configuration	M_s (kN·m)		
BR6	21.6	44226	4 tendons, each has 17-0.6” diam. strand, $f_{pti}=0.5f_{ptk}$	22622	5 rows of US #11 rebar, each row has 3 bars	17945	3676	0.68
BR9	32.4	47640	Same as above	22061	6 rows of US #11 rebar, each row has 3 bars	20415	5377	0.74
BR12	43.2	45448	Same as above	21903	Same as above	19862	7118	0.68

Note: example for wall ID, BR6 represents 6-story walls with base rocking joint only; H_w is wall height; M_{DES} is the design moment at wall base; M_p, M_s, M_g are the moment contributions from PT steel, ED steel and gravity loads, respectively; κ is the relative moment ratio as defined in the previous study; Steel area of 0.6” dima. strand and US #11 rebar are 140 mm^2 and 1006 mm^2, respectively; f_{pti} and f_{ptk} (1860 MPa) are the initial and ultimate strength of PT steel, respectively.

2.3 Earthquake ground motions

The prototype walls were subjected to a set of 20 ground motion records (10 events, each has two components) as listed in **Table 2**. This ground motion suite is part of the suggested far-field ground motion set as presented in FEMA P695 [26], which can be directly downloaded from PEER-NGA database. To scale each original ground motion for the analysis, a 5% damped spectral acceleration at the fundamental period of the structure, denoted as $S_a(T_1,5\%)$, is selected as the intensity measure for the ground motion. Individual ground motion record in the set is scaled up or down to match the target $S_a(T_1,5\%)$ from the seismic design spectrum. Although many other ground motion scaling methods could be found in literature, the one selected in this study is simple and could be easily implemented in analysis. As noted earlier, during the analysis, both DBE and MCE earthquake intensity levels have been considered, however only the MCE results would be addressed later in this paper for brief.

Table 2 – List of ground motions used in the study (from FEMA P695)

Earthquake				Scale factor (DBE)		Scale factor (MCE)	
Name (year, station)	Comp. 1	Comp. 2	PGA_{max} (g)	Comp. 1	Comp. 2	Comp. 1	Comp. 2
Northridge (1994, Beverly Hills)	MUL009	MUL279	0.52	1.14	0.88	1.71	1.31
Hector Mine (1999, Hector)	HEC000	HEC090	0.34	2.95	2.12	4.43	3.18
Imperial Valley (1979, El Centro)	E11140	E11230	0.38	2.19	1.86	3.28	2.79
Kobe (1995, Nishi-Akashi)	NIS000	NIS090	0.51	1.11	1.01	1.67	1.52
Kocaeli (1999, Duzce)	DZC180	DZC270	0.36	1.43	1.52	2.14	2.28
Landers (1992, Yermo Fire)	YER270	YER360	0.24	1.74	3.91	2.60	5.87
Loma Prieta (1989, Capitola)	CAP000	CAP090	0.53	0.96	0.72	1.44	1.08
Manjil (1990, Abbar)	ABBAR-L	ABBAR-T	0.51	1.31	1.84	1.97	2.76
Chi-Chi (1999, TCU045)	TCU045-E	TCU045-N	0.51	1.07	1.20	1.60	1.80
Friuli (1976, Tolmezzo)	TMZ000	TMZ270	0.35	3.30	0.95	4.95	1.43

Note: the scale factors listed are only for the 6-story buildings as an example.

3. Numerical modeling

Many different numerical models have been developed for self-centering wall systems during the past decades [5, 10]. Among those, fiber model is widely recognized by researchers due to its balance between precision and effectiveness. However, fiber models are still time consuming when conducting a large amount of analyses, such as parametric analyses considering several parameter variations which results too many analytical cases. Also, fiber models would be unnecessarily complicated when only the influence of the overall design parameters need to be considered. For this reason, a simple lumped mass spring model is adopted here for simulating the self-centering walls with multiple rocking joints. The software used to implement the numerical model is OpenSees [27].

Fig. 3 shows the schematic of an example 6-story self-centering wall with rocking joints at base and at the third story level. As shown, the model is a simple MDOF model with lumped mass concentrated at each floor level. The nodes representing each story are connected using elastic beam column element. At the rocking joint, a simple bi-linear hysteretic model (SelfCentering Material in OpenSees) incorporating self-centering characteristics is used to represent the moment-rotation relationship for the rocking joint behavior. As shown in the figure, the hysteretic model has four parameter inputs, namely M_y, K_1, K_2, and β, representing the yielding moment capacity, initial and second stiffness, and energy dissipation levels.

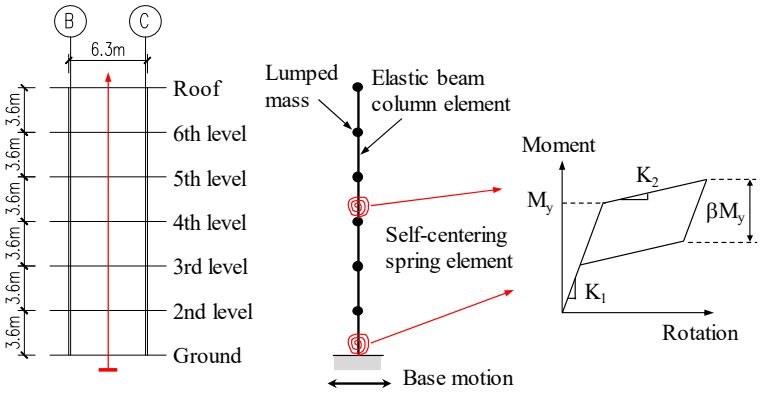

Fig. 3 – OpenSees model for self-centering walls with multiple rocking joints

As mentioned earlier, detailed wall section designs have been conducted in the previous section (for base rocking joints), and those designs were used to construct fiber models firstly. Modeling of self-centering walls using fiber models have been addressed and extensively verified otherwise [22], hence not included again. The main purpose of establishing fiber model is to calibrate the simple spring model used in this study, specifically to calibrate the SelfCentering Material model. **Fig. 4** shows a comparison of the cyclic loading responses from the fiber model and spring model. It can be seen from **Fig. 4**(a) that both the fiber model and simple model represents good base shear resistance from the force-based design. The simple spring model represents the backbone curve of the force-displacement relationship in an excellent extent, while the degrading behavior is somewhat deviated from the fiber model due to the simplicity of the hysteretic rule.

For the three prototype buildings with different heights (6-, 9- and 12-story), the design base moment capacity is quite close (**Table 1**). Hence, to simplify the modeling cases, all the models used in the current study have the same modeling parameters for the base rocking joint. The parameters for the upper rocking joints are then changed based on that for the base rocking joint. **Fig. 4**(b) shows the effects of energy dissipation parameter β in the spring model to the cyclic hysteretic response.

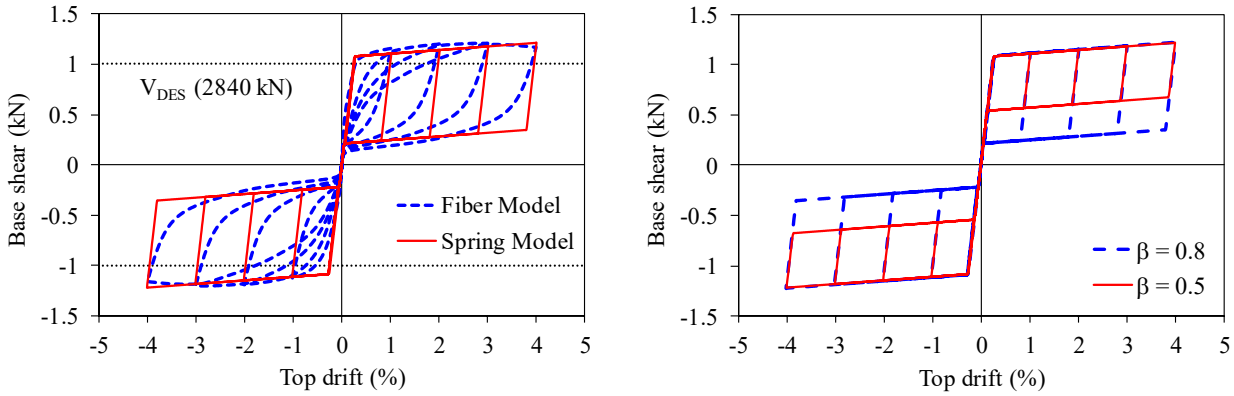

(a) Comparison of fiber model and spring model

(b) Spring model with different energy dissipation levels

Fig. 4 – Verification of the simple spring model

4. Parametric study

4.1 Parameter variation setup

The variation of the design parameter inputs (spring model) for the current study is summarized in **Table 3**. As shown in the table, the parameter variation includes: different wall heights (6-, 9- and 12-story); models with only base rocking (BR) joint cases and multiple rocking (MR) cases, and the locations and numbers of the upper rocking joints (12-story wall only) also varies; yielding moment capacity of the upper rocking joint, M_y; energy dissipation level of the upper rocking joint, β. Note that the values for M_y in **Table 3** are relative to the base moment capacity of the baseline model (represented by $M_y = 1.0$).

4.2 Effects of adding second rocking joints

Fig. 5 presents the median of the peak story moments (normalized by M_{DES} as in **Table 1**) from 20 ground motions for all the three prototype buildings with both base only rocking joints and with additional upper story rocking joints. It can be seen from the figure that all the upper rocking joints are effective in reducing the upper story moment demand. For the 6-story building, the moment control mechanism is effective for the stories below the second rocking joint (i.e., below the 3rd story for MR6), while moment amplification occurs to the higher stories above the second rocking joint. For the taller walls (6- and 9-story), the mitigation effects are more obvious in the lower stories, while the amplification effects in the upper floors are negligible. Effects of different rocking locations are not significantly evident in the study.

Fig. 6 presents the ratios for the moment of walls with multiple rocking joint (M_{MR}) and moment of walls with only base rocking joint (M_{BR}). It can be clearly seen from the figure, using multiple rocking joint mechanism to control forces in self-centering walls are significantly more effective for taller buildings (e.g., for 12-story case, this effect could be as large as 35% reduction in the moment envelope as compared to only base rocking case). For lower buildings (such as 6-story building in this case), utilize of multiple rocking joints should be cautiously evaluated.

Table 3 – Parameter variation in the study

Parametric models		Rocking joint locations	M_y (normalized by moment yielding capacity at wall base)	β (upper rocking joint)
6-story	BR6	@Base	–	–
	MR6	@Base, **@3**	**1.0**, 0.7, 0.5	**0.8**, 0.5, 0.2
9-story	BR9	@Base	–	–
	MR9	@Base, @3, **@4**	**1.0**, 0.7, 0.5	**0.8**, 0.5, 0.2
12-story	BR12	@Base	–	–
	MR12	@Base, @4, **@5**, @6, @4 and 7 (two upper rocking joints)	**1.0**, 0.7, 0.5	**0.8**, 0.5, 0.2

Note: the bold represents the baseline model parameters.

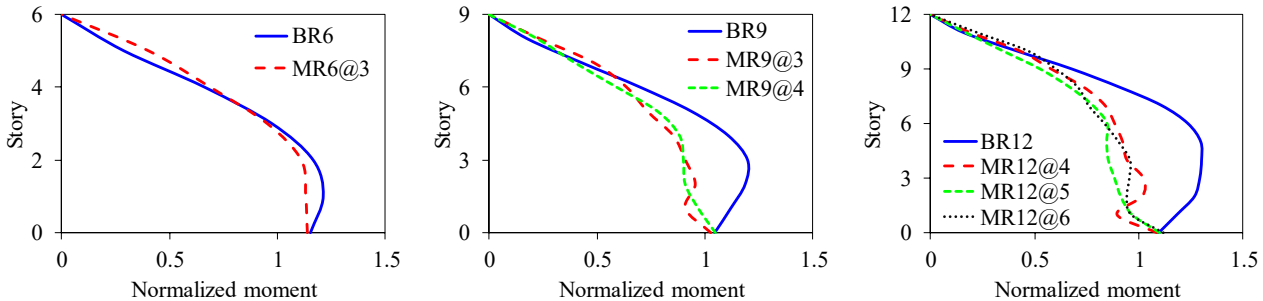

Fig. 5 – Median maximum moment envelopes for walls with only base rocking joint and with additional rocking joints at different heights

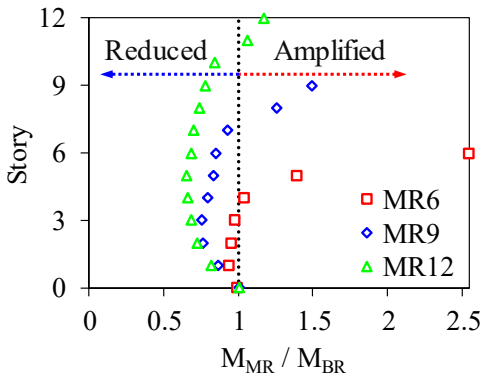

Fig. 6 – Ratio of story moment between walls with multiple and base only rocking joints

4.3 Effects of using multiple upper-story rocking joints

For taller buildings, such as the 12-story building in this study (maybe not tall enough, higher walls are needed in future study), using more than one upper-story rocking joints may be useful to further control the seismic response of taller self-centering wall systems. **Fig. 7** shows the results of using two upper-story rocking joints (at the 4th and the 7th story, respectively). As shown, the story moment over the wall height could be further reduced when introducing the second upper-story rocking joint at the 7th story as compared to using only one upper-story rocking joint at the 4th story. However, the shear control is not obvious in this study (further check for modeling of wall shear behavior is needed).

Fig. 7(c) shows the story drift envelopes for the 12-story walls with different rocking joint designs. The results reveal that using upper story rocking mechanism may cause an abrupt drift enlargement at the rocking joint story (at the 4th and 7th story). Furthermore, employing the second upper story joint (case MR12@4,7) could potentially help reducing drifts in the upper stories, while amplifying the drifts in lower stories (as compared to case MR12@4). However, this conclusion may need further verification with more analyses results included.

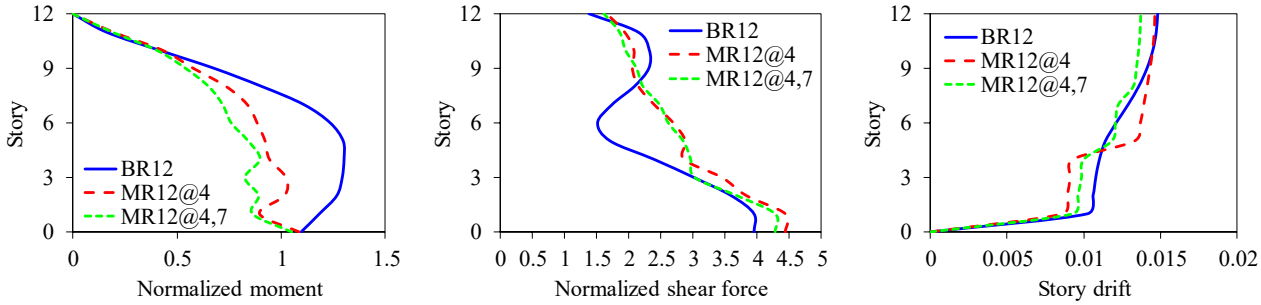

(a) Moment (b) Story shear force (c) Story drift

Fig. 7 – Impacts of introducing second upper rocking joint to the response of 12-story walls

4.4 Influence of yielding moment capacity for the upper rocking joints

In addition to the locations and numbers of upper rocking joints, the design properties for the rocking joint itself might also be critical in controlling the response of such wall system. **Fig. 8** shows the influence of yielding moment capacity M_y of the upper-story rocking joint. It can be clearly seen from the figure that reducing M_y could be effective in controlling the moment demand, and the effect is especially obvious for the stories near where the upper rocking joint locates.

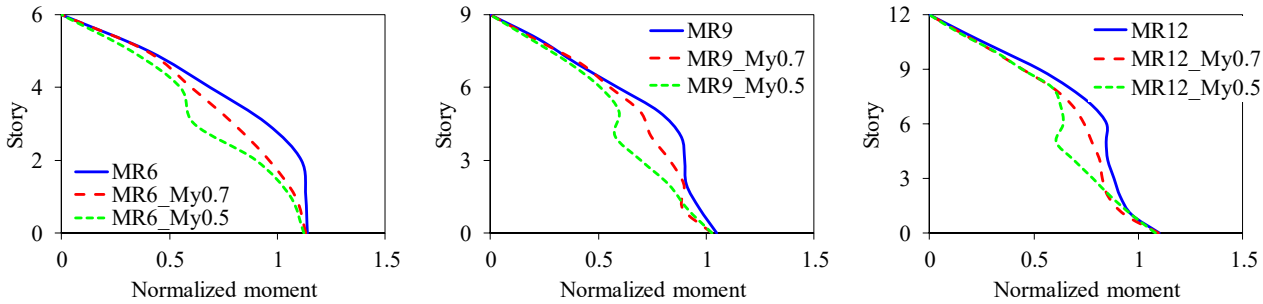

(a) 6-story (b) 9-story (c) 12-story

Fig. 8 – Influence of yielding moment capacity of upper rocking joint to the moment envelopes

While the moment mitigation is effective for rocking joint with smaller yielding capacity, the drift demand above the rocking joint may be amplified when the moment capacity is reduced. **Fig. 9** has clearly exhibited this influence by presenting the drift envelops. It can be seen from the figure, for the case walls with 50% less of the yielding moment capacity at the upper-story rocking joint (i.e., $M_y0.5$), the structure

exhibits the most obvious and abrupt drift amplification. For the cases in this study, this enlargement could be even larger than the drift demand at the 1st story which is mainly caused by the concentrated gap opening deformation resulted from base rocking mechanism. This means the yielding capacity for the upper-story rocking joint should not be reduced too much, preventing a significantly large and abruptly amplified lateral drift at the upper rocking joint locations.

Fig. 10 further displays the correlation between the maximum values of moment reduction and the drift amplification for the upper stories of 6-, 9- and 12-story walls with the moment yielding capacity level. Note that the responses in the longitudinal coordinate of the figure are normalized to the response at wall base. This figure further indicates that both the effects of moment reduction and drift amplification tend to be more evident to the taller walls than to the lower walls.

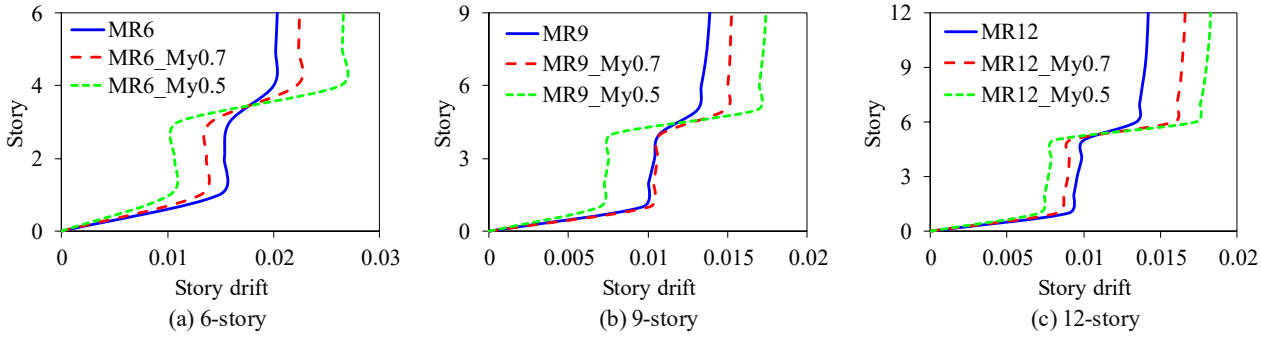

Fig. 9 – Influence of yielding moment capacity of upper rocking joint to the story drift envelopes

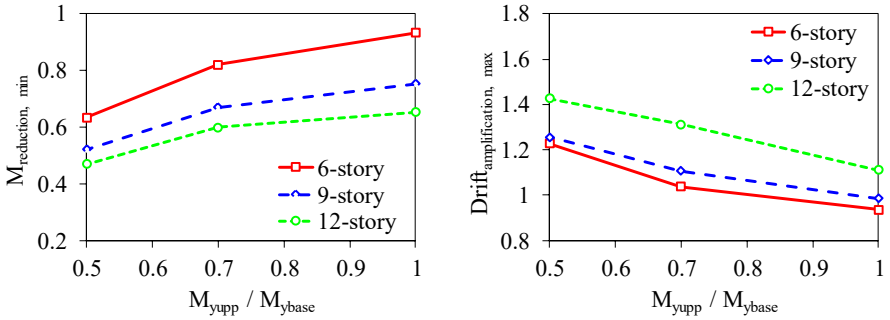

Fig. 10 – Correlation between yielding moment capacity of upper rocking joints and the overall structural response

4.5 Influence of energy dissipation levels for the upper rocking joints

Fig. 11 and **Fig. 12** presents similar results for the story moment and drift distribution when considering various upper story energy dissipation levels. From the cases in this study, the influence of energy dissipation levels (β) to the wall response is not evident for controlling the wall responses, both for the moment and drift demand. A possible reason to explain this phenomenon is that the response of such system is mainly controlled by rocking mechanism. This conclusion should be further investigated in future.

Fig. 13 further displays the correlation between the maximum values of moment reduction and the drift amplification for the upper stories of 6-, 9- and 12-story walls with the energy dissipation levels of the upper rocking joints. The figure again indicates that the effects of moment reduction and drift amplification are more evident to the taller walls than to the lower walls.

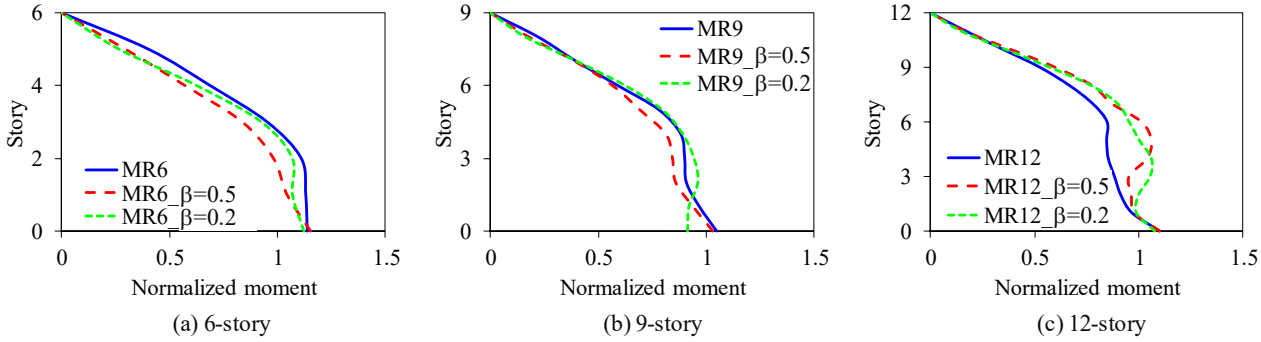

Fig. 11 – Influence of energy dissipation level of upper rocking joint to moment envelopes

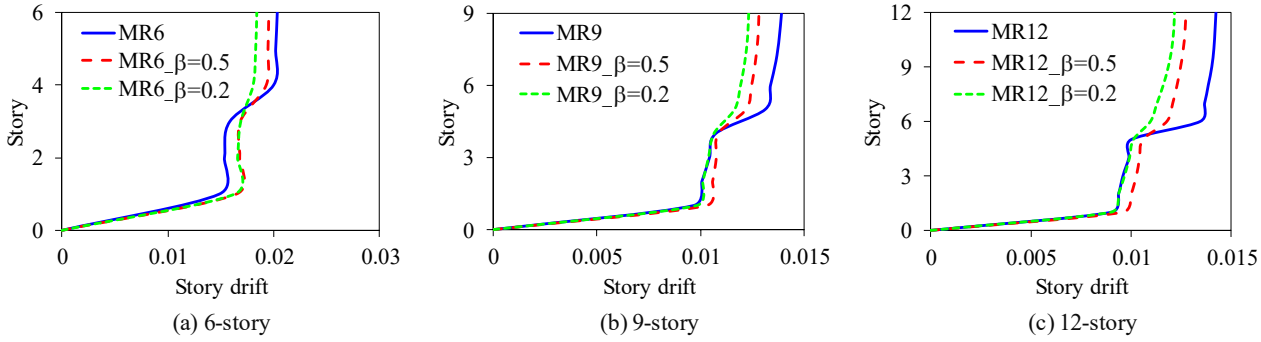

Fig. 12 – Influence of energy dissipation level of upper rocking joint to story drifts

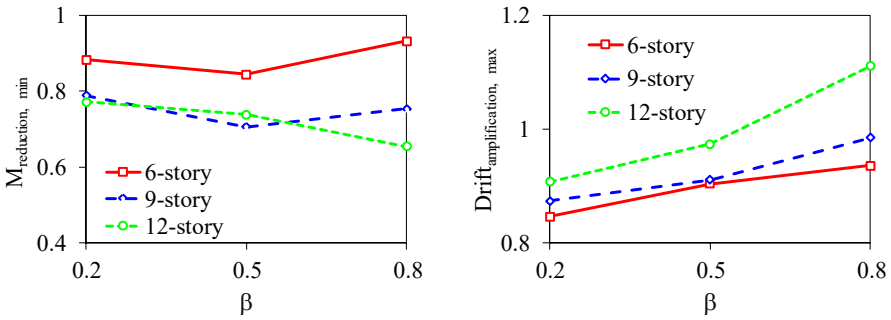

Fig. 13 – Correlation between energy dissipation level of upper rocking joints and the overall structural responses

5. Conclusions

This paper presents a parametric analysis for the self-centering precast walls using multiple rocking joints. Three prototype walls with different critical design parameters are designed. The variation of the design parameters includes: wall heights, rocking joint locations and numbers, yielding capacities of upper rocking joint, energy dissipation levels of upper rocking joint. The following conclusions could be drawn from the study:

(1) In addition to base rocking joint, the utilization of upper-story rocking joints is effective in reducing wall force demand in upper wall panels. This mitigation effect is much obvious for taller wall cases than that in lower walls. The effects of different rocking joint locations to the overall response is not significantly evident in this study. More studies need to be conducted in order to position an optimal location for the upper story rocking joint.

(2) Multiple rocking joint mechanism to control forces in self-centering walls are significantly more effective for taller walls. For lower walls, using multiple rocking joints should be cautiously evaluated.

(3) Using multiple upper story rocking joints is effective to further mitigate the force demands in taller walls. However, this may cause an abrupt drift enlargement near the story where the rocking joint locates.

(4) Reducing yielding moment capacity for the upper-story rocking joint is effective in controlling the moment demand. However, the drift demand above the rocking joint may also be amplified. This indicates that the upper-story moment capacity should not be overly reduced, in order to prevent a significantly large and abruptly amplified story drift in the upper stories. Furthermore, both the effects of moment reduction and drift amplification tend to be more obvious to the taller walls than the lower walls.

(5) From the case walls in this study, the influence of energy dissipation levels for the upper rocking joint is not evident for controlling the wall responses. However, more studies need to be conducted in future to verify this conclusion.

6. Acknowledgements

This research is supported by the National Natural Science Foundation of China (Grant No. 51908429 and 51938013) and the Key Laboratory of Earthquake Engineering and Engineering Vibration, Institute of Engineering Mechanics, China Earthquake Administration (Grant No. 2019D11). The authors appreciate the supports from the organizations addressed above.

7. References

[1] Priestley MJN (1991): Overview of PRESSS research program. *PCI Journal*, 36(4), 50-57.
[2] Priestley MJN, Sritharan S, Conley JR, Pampanin S (1999): Preliminary results and conclusions from the PRESSS five-story precast concrete test building. *PCI Journal*, 44(6), 42-67.
[3] Lu X, Chen Y, Mao Y (2011): New concept of structural seismic design: earthquake resilient structures. *Journal of Tongji University (Natural Science)*, 39(7), 941-947. (in Chinese)
[4] Kurama YC, Pessiki S, Sause R, Lu LW (1999): Seismic behavior and design of unbonded post-tensioned precast concrete walls. *PCI Journal*, 44(3): 72-89.
[5] Perez FJ, Sause R, Pessiki S (2007): Analytical and experimental lateral load behavior of unbonded posttensioned precast concrete walls. *Journal of Structural Engineering*, 133(11): 1531-1540.
[6] Restrepo JI, Rahman A (2007): Seismic performance of self-centering structural walls incorporating energy dissipators. *Journal of Structural Engineering*, 133(11): 1560-1570.
[7] Lu XL, Wu H (2017): Study on seismic performance of prestressed precast concrete walls through cyclic lateral loading test. *Magazine of Concrete Research*, 69(17): 878-891.
[8] Perez FJ, Pessiki S, Sause R (2013): Experimental lateral load response of unbonded post-tensioned precast concrete walls. *ACI Structural Journal*, 110(6): 1045-1056.
[9] Smith BJ, Kurama YC, McGinnis MJ (2011): Design and measured behavior of a hybrid precast concrete wall specimen for seismic regions. *Journal of Structural Engineering*, 137(10): 1052-1062.
[10] Smith BJ, Kurama YC, McGinnis MJ (2013): Behavior of precast concrete shear walls for seismic regions: comparison of hybrid and emulative specimens. *Journal of Structural Engineering*, 139(11): 1917-1927.
[11] Kurama YC (2000): Seismic design of unbonded post-tensioned precast walls with supplemental viscous damping. *ACI Structural Journal*, 97(4): 648-658.
[12] Holden T, Restrepo J, Mander JB (2003): Seismic performance of precast reinforced and prestressed concrete walls. *Journal of Structural Engineering*, 129(3): 286-296.
[13] Marriott D, Pampanin S, Bull D (2008): Dynamic testing of precast, post-tensioned rocking wall systems with alternative dissipating solutions. *Bulletin of the New Zealand Society for Earthquake Engineering*, 41(2): 90-103.
[14] Twigdena KM, Henry RS (2019): Shake table testing of unbonded post-tensioned concrete walls with and without additional energy dissipation. *Soil Dynamics and Earthquake Engineering*, 119: 375-389.
[15] Nazari M, Sritharan S (2018): Dynamic evaluation of PreWEC systems with varying hysteretic energy dissipation. *Journal of Structural Engineering*, 144(10): 04018185.
[16] Gavridou S, Wallace JW, Nagae T, Matsumori T, Tahara K, Fukuyama K (2017): Shake-table test of a full-scale 4-story precast concrete building. I: overview and experimental results. *Journal of Structural Engineering*, 143(6): 04017034.

[17] Priestley MJN, Amaris AD (2002): Dynamic amplification of seismic moments and shear forces in cantilever walls, *Research Report ROSE-2002/01*, IUSS Press, Pavia, Italy.
[18] Panagiotou M, Restrepo JI (2009): Dual-plastic hinge design concept for reducing higher-mode effects on high-rise cantilever wall buildings. *Earthquake Engineering & Structural Dynamics*, 38(12): 1359-1380.
[19] Wiebe L, Christopoulos C (2009): Mitigation of higher mode effects in base-rocking systems by using multiple rocking sections. *Journal of Earthquake Engineering*, 83-108.
[20] Schoettler MJ, Belleri A, Zhang DC, Restrepo JI, Fleischman RB (2009): Preliminary results of the shake-table testing for the development of a diaphragm seismic design methodology. *PCI Journal*, 54(1): 100-124.
[21] Henry RS, Ingham JM, Sritharan S (2012): Wall-to-floor interaction in concrete buildings with rocking wall systems. *Proceedings of the 2012 NZSEE Annual Conference*, Christchurch, New Zealand.
[22] Wu H, Zhou Y, Liu W (2019): Collapse fragility analysis of self-centering precast concrete walls with different post-tensioning and energy dissipation designs. *Bulletin of Earthquake Engineering*, 17(6): 3593-3613.
[23] ASCE (2010): Minimum design loads for buildings and other structures (ASCE/SEI 7-10). *American Society of Civil Engineers*, Reston, VA.
[24] ACI (2009): Design of a special unbonded post-tensioned precast shear wall satisfying ACI ITG-5.2 requirements (ACI ITG-5.2-09). *ACI Innovation Task group 5*, Farmington Hills, MI.
[25] ACI (2014): Building code requirements for structural concrete (ACI 318-14) and commentary on building code requirements for structural concrete (ACI 318R-14). *ACI Committee 318*, Farmington Hills, MI.
[26] FEMA (2009): Quantification of building seismic performance factors. *Federal Emergency Management Agency*, Washington, DC.
[27] Mazzoni S, McKenna F, Scott MH, Fenves GL (2016): Open system for earthquake engineering simulation (OpenSees) command language manual, *Pacific Earthquake Engineering Research Center*, University of California, Berkeley, CA.

